Robust predictions of the interacting boson approximation model

R. F. Casten,[1,2] P. von Brentano,[2] and N. V. Zamfir[1,2,3,4]
[1]*Brookhaven National Laboratory, Upton, New York 11973*
[2]*Institut für Kernphysik, University of Köln, Köln, D-50937 Germany*
[3]*Clark University, Worcester, Massachusetts 01610*
[4]*Institute of Atomic Physics, Bucharest Magurele, Romania*
(Received 6 October 1993)

The interacting boson approximation (IBA) model has existed for nearly twenty years and has now entered the lexicon of standard nuclear models used to interpret data on low-energy nuclear structure. While most recognized for its symmetries and algebraic structure, the model has a number of other less-well-known but equally intrinsic properties which give *unavoidable*, parameter-free predictions. Since these predictions cannot be altered and since they concern central aspects of low-energy nuclear collective structure, they provide a set of basic tests of the inherent framework of the model. This paper outlines these "robust" predictions and compares them with the data.

PACS number(s): 21.60.Ev, 21.60.Fw, 21.10.Re

I. INTRODUCTION

The interacting boson approximation (IBA) model [1,2], proposed in 1974, is now nearly 20 years old and has undergone many tests [3–6]. Along with some refinements and extensions to it, the model has now entered the standard lexicon of models that form the base for the interpretation of low-energy nuclear structure. Although the IBA is primarily macroscopic, it also has an important and essential microscopic aspect through its explicit inclusion of the finite number of valence nucleons. Thus its niche is intermediate between the shell model and macroscopic collective models. It looks to the one for its microscopic justification and to the other for its geometrical interpretation.

While the dynamical symmetries and algebraic structure of the IBA are its best known characteristics, there are a number of other aspects that are equally intrinsic to the model. Many of these are in the nature of "inherent" or "automatic" predictions of the IBA in the sense that they are parameter free (or nearly so with any reasonable set of parameters): *were the data to be different it would be virtually impossible to alter the model to accommodate them.* They reflect the intrinsic structure of the model and relate to very basic aspects of collectivity in nuclei. We call these "robust" predictions. Thus, they comprise a set of tests of the basic relevance of the model to low-energy nuclear structure.

It is the purpose of this paper to discuss these robust properties of the IBA and their comparison with the data. Our discussion deals with the IBA-1. We neglect the IBA-2 [7] with its interesting ideas of F-spin symmetry [8] and F-spin multiplets [9], $M1$ collective modes [10], and the like. The basic predictions of the IBA discussed below are generally not new, but a number have never been explicitly compared with the data, or only have done so with fragmentary data. We have carried out a more thorough scan of the literature in order to collect and display this scattered information and lay out a compact survey of these inherent properties of the IBA and their comparison with experiment.

II. GENERAL ASPECTS OF THE IBA

Of course, the IBA's most recognized property has always been its dynamical symmetries, which emerge naturally from its algebraic structure and, in particular, from its founding in the U(6) group. For the IBA-1, these symmetries are U(5), SU(3), and O(6), which correspond geometrically to an anharmonic vibrator, a particular type of symmetric rotor (characterized, for example, by degenerate β and γ bands), and to a deformed completely γ-soft vibrator (closely linked to the Wilets-Jean model), respectively. Indeed, historically, the prediction [2] of the O(6) symmetry, which accounts for literally dozens of $E2$ branching ratios and for extensive energy patterns, prior to its empirical discovery [3,11] in the Pt and Xe-Ba regions, marked a key point in the acceptance of the model as a viable alternative description. And, the U(5) and SU(3) symmetries of the IBA provide group theoretical versions of their familiar phenomenological counterparts in which all intrinsic excitations (e.g., β, γ bands, multiphonon states) are linked in unified frameworks.

Related to the limiting symmetries themselves is the simplicity of the phase/shape transitional regions that connect them: these structural changes are accomplished by varying only one or two parameters in the IBA. Moreover, these parameters have simple physical significance. An intriguing result [12] is that of all possible "trajectories" between symmetries, real nuclei seem to reflect the simplest routes in the IBA, namely, those with very smooth (indeed, often nearly linear) variations of the parameters. Why it is that the simplest IBA trajectories reflect empirical behavior is an important microscopic issue.

Equally interesting are other "global" results. For example, the detailed IBA parameters required to fit dif-

ferent deformed nuclei vary very little. Indeed, one can almost define a "standard" IBA-1 calculation [6] for deformed nuclei in which a good part of the variations in predicted properties from nucleus to nucleus arises from variations in boson number alone.

The IBA-1 has also been extended to negative-parity states by incorporating $p(L = 1)$ and $f(L = 3)$ bosons [2]. Here again, a number of simple results arise. For example, incorporating an f boson, the energy ordering of the $K^\pi = 0^-$, 1^-, 2^-, and 3^- bands in deformed nuclei depends only on one parameter, called F_2, which is the ratio of exchange to quadrupole $[Q_d \cdot Q_f]$ terms in the *sdf* part of the Hamiltonian [13]. F_2 reflects the location of the Fermi surface (the fractional filling of a shell). The predicted K-band ordering varies with F_2 from that listed above to nearly its inverse and is in agreement with the well-known empirical systematics. Finally, the systematic changes in $B(E1)$ values connecting negative-parity states to the positive-parity yrast levels are easily explained [14] by smooth trends in the parameters.

The inclusion within the model structure of its three symmetries, of transitional regions and intermediate structures, all in a single framework allowing easy calculation of many nuclear observables, is in itself a very appealing aspect. It means that the model spans and unifies virtually all of the empirical manifestations of collectivity in low-lying nuclear spectra, and this universality has facilitated its frequent and extensive comparison with experiment.

III. SPECIFIC ISSUES

All this history, however, is well known–our purpose here is rather to highlight lesser known predictions which are no less inherent to the model (and which were often previously unexpected). Many of them stem from the explicit inclusion of finite valence nucleon number (boson number, N_B) in the model. Along with its symmetries, this feature is one of the two key ingredients that distinguish the model from most others. While sometimes viewed as a limitation of the model, it is actually one of the model's strengths. Although superficially it seems to limit the applicability of the model for high spin states, it is more likely that such states involve the degrees of freedom outside the standard *s-d* IBA-1, such as two quasiparticles coupled to the IBA core, or amplitudes for g ($L = 4$), or higher angular momentum, bosons, or even effective shell spaces (effective N_B values). In fact, though, the explicit inclusion of finite boson number is one of the critical aspects of the IBA that leads to numerous predictions of collective behavior and its systematics that are in agreement with the data. Many of these predictions are difficult to obtain with other models, especially with macroscopic geometrical models which usually do not automatically relate predictions of one nucleus with those of adjacent ones since the predictions must be "self-parametrized" for each nucleus. Of course, other valence models [15] such as symplectic models or the fermion dynamical symmetry model may contain predictions analogous to some of those below, and it would be interesting to see these delineated.

In the following paragraphs these automatic and robust predictions of the IBA are grouped and discussed under a couple of general headings. We start with the well-known property of collective nuclei, namely, the rapid increase in $B(E2{:}0_1^+ \rightarrow 2_1^+)$ values toward midshell. We then turn to a number of other more subtle and less known, but important and characteristic, aspects of nuclear structure associated with the basic shape and structure of collective nuclei (e.g., γ values, γ softness, and rotation-vibration coupling), and with the nature of the elementary collective excitation modes (especially β and γ vibrations) which they exhibit. In each case, the IBA makes ineluctable predictions, and we compare these with the empirical situation.

A. Mean field collectivity

First, we consider the yrast levels themselves, reflective of the mean field structure. An excellent measure of this structure is the $B(E2)$ value to the first 2^+ state. Generally, in algebraic valence models, this $B(E2)$ is expected to increase toward midshell due to the increase in valence nucleon number and the increase in the quantum numbers labeling the group representations involved. In the IBA the prediction of a strong increase in $B(E2{:}0_1^+ \rightarrow 2_1^+)$ values in deformed nuclei, with increasing valence proton and neutron numbers (increasing boson number), is virtually independent of any parameter variations. The specific N_B dependence of these $B(E2)$ values for deformed nuclei in the IBA is a direct reflection of two aspects of finite N_B, namely, the finite value itself and the partition of N_B bosons into n_s s bosons and n_d d bosons, both of which increase with N_B for low-lying levels. In deformed nuclei, each factor in the (dominant) $(s^\dagger d + d^\dagger s)$ term in the $E2$ operator essentially gives a power of N_B, leading to an approximate N_B^2 dependence. In particular, in the SU(3) limit, $B(E2{:}0_1^+ \rightarrow 2_1^+) \propto (2N_B + 3)N_B$.

Such a behavior is very well-known empirically, as shown for $B(E2{:}0_1^+ \rightarrow 2_1^+)$ values [16] on the left in Fig. 1. On the right are the SU(3) predictions. Different assumptions for the detailed N_B dependence, such as invoking a transition between U(5) and SU(3), or a broken-SU(3) structure, would produce predictions that are qualitatively (and nearly quantitatively) the same. The predicted systematics, including the increase toward midshell, is very similar to that seen in the data. The IBA, through its explicit inclusion of the number of valence nucleons, thus automatically accounts for the growth of collectivity toward midshell. The main difference between the IBA and experiment is that the latter exhibits a well-known saturation effect near midshell which is Pauli effect related and beyond the scope of the IBA-1. An interesting open issue for the yrast states, possibly related to boson number, is the treatment of the higher spin levels where $B(E2{:}J \rightarrow J-2)$ values are predicted to fall off with increasing J whereas such falloffs are seldom observed.

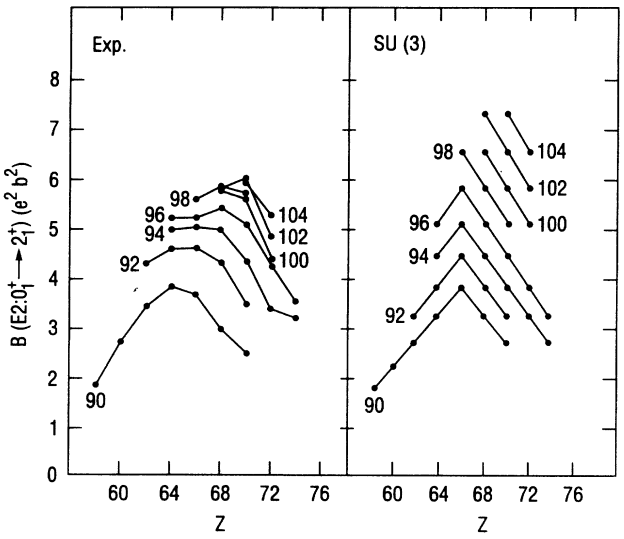

FIG. 1. Empirical and calculated $B(E2: 0_1^+ \rightarrow 2_1^+)$ values. The calculations are carried out in the SU(3) limit with constant effective charge. The inherent N_B dependence of these $B(E2)$ values for deformed nuclei in the IBA gives the predicted rise toward midshell. The data are taken from Ref. [16].

B. Axial asymmetry

1. *Gamma softness versus rigidity*

Axially asymmetric nuclei in the IBA-1 are always γ soft. As shown in Fig. 2, the IBA potential either has no minimum [the O(6) extreme of a γ-flat potential ($\chi = 0$) with $\gamma_{eff} \sim 30°$] or a minimum at 0°. There are no minima for $\gamma \neq 0°$. For IBA potentials with a minimum at $\gamma = 0°$, the steepness increases with boson number. Hence, strict axial symmetry can only occur in the infinite N_B limit, and finite γ values arise only from zero point motion in a γ-soft potential. This is inherent in the *s-d* boson structure of the IBA space and in the form of the IBA Hamiltonian which includes terms up to second order in the boson creation and destruction operators. Of course, inclusion of higher order terms [e.g., "cubic" terms of the form $\theta_3(d^\dagger d^\dagger d^\dagger)^{(3)}(ddd)^{(3)}$] do give a contribution to the potential with a minimum at finite γ, but such terms (mentioned briefly again below) are an extension to the original IBA and are not considered explicitly here. Thus, the *s-d* IBA-1 corresponds to the opposite picture of the origin of axial asymmetry as the rigid triaxial Davydov [18] model.

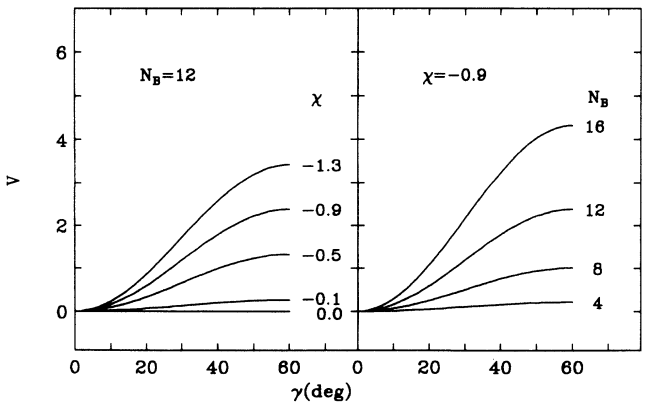

FIG. 2. The IBA potential $V(\gamma)$ vs γ. Arbitrary units. Based on Ref. [17]. Left side, for several values of χ with fixed N_B. Right side, for several N_B values with constant χ.

These properties of the IBA can be tested experimentally by using the energy staggering in the γ band as a signature of γ softness or rigidity. In a γ-soft potential, the quasi γ-band levels cluster in energy couplets as $2^+, (3^+, 4^+), (5^+, 6^+), \ldots$ whereas in a γ-rigid potential the clustering goes as $(2^+, 3^+), (4^+, 5^+), \ldots$. A sensitive signature is therefore the staggering index

$$S(\gamma) = \frac{[E(4_\gamma^+) - E(3_\gamma^+)] - [E(3_\gamma^+) - E(2_\gamma^+)]}{E(2_1^+)} - 0.33. \quad (1)$$

$S(\gamma)$ is defined so that the symmetric rotor limit corresponds to $S(\gamma) = 0$. (This definition differs from that of Ref. [19] only in the presence of the additive constant -0.33. Analogous $S(\gamma)$ values can be defined for other spins: the constant, -0.33, remains the same.) Empirical $S(\gamma)$ values for all even-even nuclei from $Z = 30$ to the actinides are shown in Fig. 3 for comparison with both IBA and Davydov model predictions. *Negative* $S(\gamma)$ values correspond to axial asymmetry which arises from γ softness in the potential and *positive* values to *γ-rigid* motion: the magnitude of $S(\gamma)$, of course, depends on the

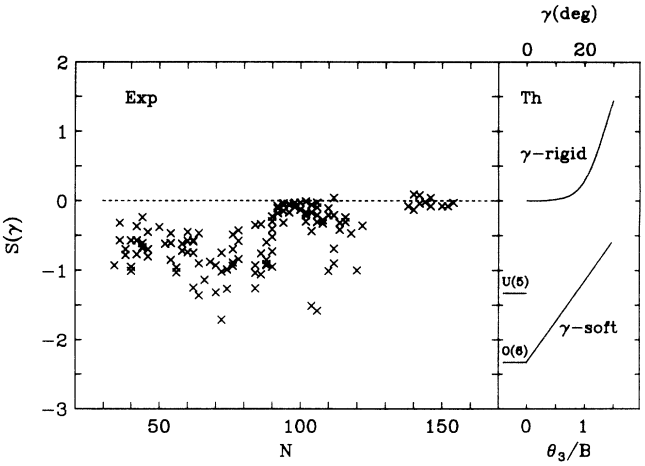

FIG. 3. Left: Empirical values of the staggering index $S(\gamma)$, defined in Eq. (1). Right: Predictions of $S(\gamma)$ are given for the γ-rigid Davydov model as a function of γ (top scale) and for the IBA in the U(5) and O(6) limits (short horizontal lines) and for O(6) as a function of θ_3/B. θ_3 specifies the contribution of a cubic term that adds a weak component with a minimum at $\gamma = 30°$ to the γ-flat O(6) potential and B is the coefficient of the $\tau(\tau + 3)$ term in the O(6) eigenvalue expression. Their ratio gives the relative importance ($\delta V/V$ ratios of a few % here) of the cubic term. The results illustrate that, empirically, low-spin nuclear axial asymmetry is invariably γ soft in accord with the geometric structure of the IBA-1. Based on Ref. [19].

value of γ at the potential minimum (for γ-rigid shapes) and on the average value of γ and the steepness of the potential for the γ-soft case. The specific (negative) values of $S(\gamma)$ in the IBA can be varied by varying the parameters of the Hamiltonian. Likewise, by introducing a very small cubic term to the IBA-1 Hamiltonian, which adds a component to the potential with a minimum at $\gamma = 30°$ (constituting at most a few % of the potential), it is also possible, as shown in the figure, to obtain a range of negative $S(\gamma)$ values. The main point in the present context, though, is that negative $S(\gamma)$ values are an unavoidable characteristic of the original IBA-1 model and positive $S(\gamma)$ values are virtually unobtainable.

Figure 3 clearly shows that, empirically, there are virtually no nuclei in the γ-rigid domain. Small negative $S(\gamma)$ values correspond to nearly axially symmetric nuclei with fairly steep potentials and minima at $\gamma = 0°$ and, consequently, rather small $\gamma_{\rm eff}$ values. These nuclei will be discussed just below in terms of rotation-vibration interactions or K mixing. More negative $S(\gamma)$ values correspond to potentials that are softer in γ: U(5) (the vibrator limit) gives $S(\gamma) = -1.33$ (recall that a spherical vibrator potential is γ flat) and O(6) gives $S(\gamma) = -2.33$. It is evident from the figure that, at least at low spin, all nuclear axial asymmetry in even-even nuclides arises from γ softness, in accord with the IBA view.

2. Band mixing

As noted, small negative $S(\gamma)$ values in the IBA correspond to well-deformed nuclei with a small rotation-vibration interaction, or, in other words, γ-band–ground-band mixing. Such mixing has been studied for decades and is expressed in terms of a band mixing parameter Z_γ which is proportional to the spin-independent part of the amplitude of the ground band in the first excited $K = 2$ band. The empirical values of Z_γ for rare-earth nuclei are shown in Fig. 4. They have been extracted from the slopes in Mikhailov plots according to the discussion in Ref. [20].

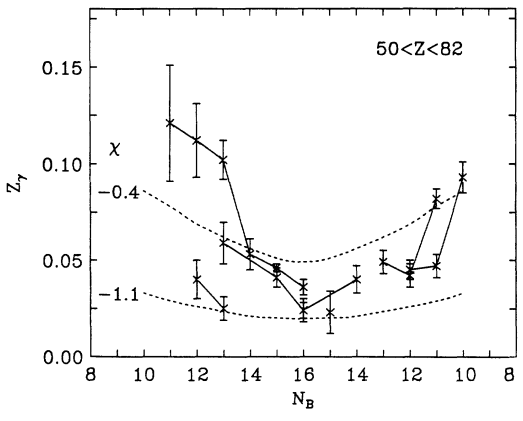

FIG. 4. Empirical Z_γ values vs N_B for rare-earth nuclei. From Ref. [20]. Z_γ is proportional to the spin-independent part of the γ-band–ground-band mixing amplitude. The dashes are IBA calculations in the CQF for two χ values that bound those used in typical calculations. These curves show a similar (but weaker) parabolic dependence on N_B as that seen in the data.

The IBA predicts that this mixing has a specific behavior across a shell, namely, that it decreases with increasing boson number. Thus Z_γ is predicted to have a roughly parabolic behavior across a shell with lowest values near midshell. This feature can be seen in a simple calculation in the consistent Q formalism [12] (CQF). The calculation uses the IBA Hamiltonian $H = -\kappa Q \cdot Q$ where $Q = s^\dagger d + d^\dagger s + \chi(d^\dagger d)^{(2)}$ in which the variation of structure from O(6) to SU(3) corresponds simply to varying χ from 0 to -1.32. The results are shown in Fig. 4 for two *fixed* values of χ that encompass the range of values encountered in realistic calculations. Even though the Hamiltonian and its parameters remain constant, the Z_γ values vary parabolically. In realistic calculations, of course, the value of χ [which is usually fixed by fitting a $\gamma \rightarrow g$ $B(E2)$ value] will vary somewhat from one deformed nucleus to the next and the steepness of the parabolas will increase, giving improved agreement with the data.

The parabolic behavior of Z_γ in the IBA arises from the interplay of symmetry structure and finite N_B effects. γ-g band mixing arises in good measure from γ-β mixing, which is a feature even of the SU(3) limit, since the β and γ bands belong to the same representation. γ-β mixing, which decreases rapidly with increasing N_B, is transmitted to γ-g band mixing via $\Delta K = 0$ β-g mixing, which is the dominant mixing that occurs when SU(3) is broken [21].

3. Gamma values for deformed nuclei

There is one other important feature of axial asymmetry where the IBA provides an inherent prediction that can be compared with the data. As suggested on the left in Fig. 2, the effective value of γ (arising from zero point motion) in the IBA is directly correlated with the parameter χ. Indeed, a $\gamma_{\rm eff}$-χ correlation can be developed [22] by comparing observables related to the γ band that are predicted by the IBA with those given by the Davydov model. (Even though the origin of $\gamma_{\rm eff}$ is different in the IBA and Davydov models, the procedure of extracting an effective $\gamma_{\rm eff}$ value by comparing certain calculated observables in the two models has been shown [23] to be valid.) In Fig. 5 this correlation is extracted from empirical values of $E(2^+_\gamma)/E(2^+_g)$ and is shown for several N_B values. Similar $\gamma_{\rm eff}$-χ correlations result if other observables [such as $B(E2)$ values involving the γ band] are used instead [22]. The figure shows a result which is perhaps at first surprising, namely, that $\gamma_{\rm eff}$ does *not* equal 0°, *even* in SU(3). As the figure suggests, only in the limit $N_B \rightarrow \infty$ does $\gamma_{\rm eff} \rightarrow 0°$. This is actually not surprising since the right side of Fig. 2 shows that, for a given χ, the potential has finite steepness for finite N_B. Thus the IBA inherently predicts that while $\gamma_{\rm eff}$ decereases with increasing N_B, realistic deformed nuclei must have nonzero $\gamma_{\rm eff}$ values. Moreover, since maximum N_B values are ~14–20, the IBA inherently predicts an actual numerical value for the minimum $\gamma_{\rm eff}$ values

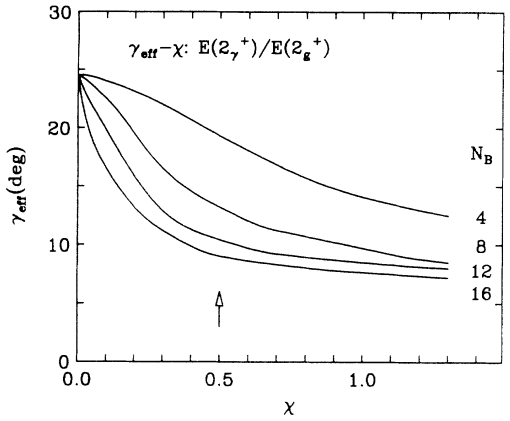

FIG. 5. γ_{eff}-χ relationship obtained by calculating $E(2_\gamma^+)/E(2_g^+)$ in the Davydov and IBA models (for several N_B values) and equating the values of γ in the former to those of χ in the latter that give the same values of this energy ratio. Note that γ_{eff} does *not* go to zero even in the SU(3) limit but remains finite at ~7–10° in accord with the data (see Fig. 6). The arrow indicates a typical χ value for deformed nuclei.

observed in deformed nuclei near midshell, namely, ~ 8°.

Empirical γ_{eff} values have traditionally been obtained [18] from the same energy ratio used to construct the theoretical plots in Fig. 5. These empirically extracted values are shown in Fig. 6 for the rare-earth region where it is indeed seen that most well-deformed nuclei have γ_{eff} values remarkably close to the IBA prediction of ~7–10°.

C. Relation of intrinsic collective β and γ modes

The lowest two positive-parity collective modes, and by far the best known, are the β and γ modes. (We use the traditional labels here, in particular the "β" label for the lowest excited $K = 0$ collective mode, although we note that the comparison of IBA and experiment is

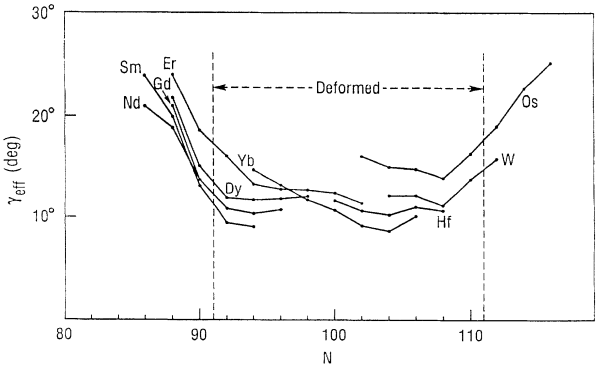

FIG. 6. Empirical values of γ_{eff} for some rare-earth nuclei obtained from $E(2_\gamma^+)/E(2_g^+)$ values. Data taken from Ref. [24]. The magnitudes of the γ_{eff} values for well-deformed nuclei ($\gamma_{\text{eff}} \sim 10°$) are in agreement with the automatic IBA predictions (see Fig. 5).

simply done for the lowest excited $K = 0$ and 2 excitations. We will also comment below a bit on the nature of the β vibration.) The IBA embodies a number of specific predictions for these modes and, very interestingly, for their relationship. These predictions have their origins in the properties of the parent SU(3) representation that contains the lowest $K = 0$ and 2 modes, and persist for realistic deformed nuclei in which SU(3) is substantially broken. As explicit calculation shows the most obvious consequence—but the most difficult to test experimentally—is that, contrary to many other models, the IBA predicts *collective* $E2$ transitions *between* β and γ bands. Indeed, in realistic deformed nuclei $B(E2{:}\beta \leftrightarrow \gamma)$ values are actually predicted to be *comparable* to $B(E2{:}\gamma \rightarrow g)$ values. In contrast, $\beta \rightarrow g$ $E2$ transitions are very weak, even when SU(3) is strongly broken for deformed nuclei.

A convenient way to show these predictions is again to exploit the CQF in which SU(3) symmetry breaking depends only on the parameter χ in the quadrupole operator. It is then possible to display a full range of predictions in terms of contour plots of appropriate $B(E2)$ or energy ratios against boson number and χ. Such contour plots are shown in Fig. 7. Figures 7(c) and 7(d) immediately give the two related, but distinct, predictions [6] just mentioned, namely,

$$B(E2:\beta \leftrightarrow \gamma) \sim B(E2:\gamma \rightarrow g) \quad \text{[Fig. 7(d)]} \qquad (2)$$

and

$$B(E2:\beta \rightarrow g) \ll B(E2:\gamma \rightarrow g) \quad \text{[Fig. 7(c)]}. \qquad (3)$$

It is evident from Fig. 7 that relations (2) and (3) are valid over the entire ranges of N_B and χ values corresponding to deformed nuclei (indeed, over much broader ranges of structure and parameters). Though their origin can be traced to the SU(3) limit, the predictions refer to the lowest $K = 0$ and 2 modes, and inspection of the wave functions shows that they are substantially mixed in terms of SU(3) representations. The predictions are truly "inherent" or robust in the sense that they would be unavoidable even if the data were the opposite.

Relation (2) was thought to be at variance with the data when it was first noted as an unavoidable result of the IBA-1 since $\beta \rightarrow \gamma$ transitions had not been observed at that time. However, it has since been recognized that this situation was an experimental artifact resulting from the weak $\beta \rightarrow \gamma$ transition *rates* (γ-ray intensities) due to the $E^5_{\gamma\text{-ray}}$ hindrance of these low-energy transitions $[(E_\beta - E_\gamma) \ll (E_\beta - E_g)]$. When sufficiently sensitive experiments were carried out, using the unique crystal spectrometers of the Institute Laue, Langevin, Grenoble, with their very-high-energy resolution and dynamic range of observable intensities, collective $\beta \leftrightarrow \gamma$ transitions were indeed found. The most famous example [5] is ^{168}Er but similar results characterize [6] the nuclei ^{152}Sm, ^{154}Gd, ^{158}Gd, ^{166}Er, and ^{178}Hf. In ^{168}Er, the ratio of reduced intrinsic matrix elements $\langle 2_\gamma^+ || E2 || 0_\beta^2 \rangle / \langle 2_\gamma^+ || E2 || 0_g^+ \rangle = 0.37$, which is somewhat smaller than the IBA prediction of ~ unity but which is an order of

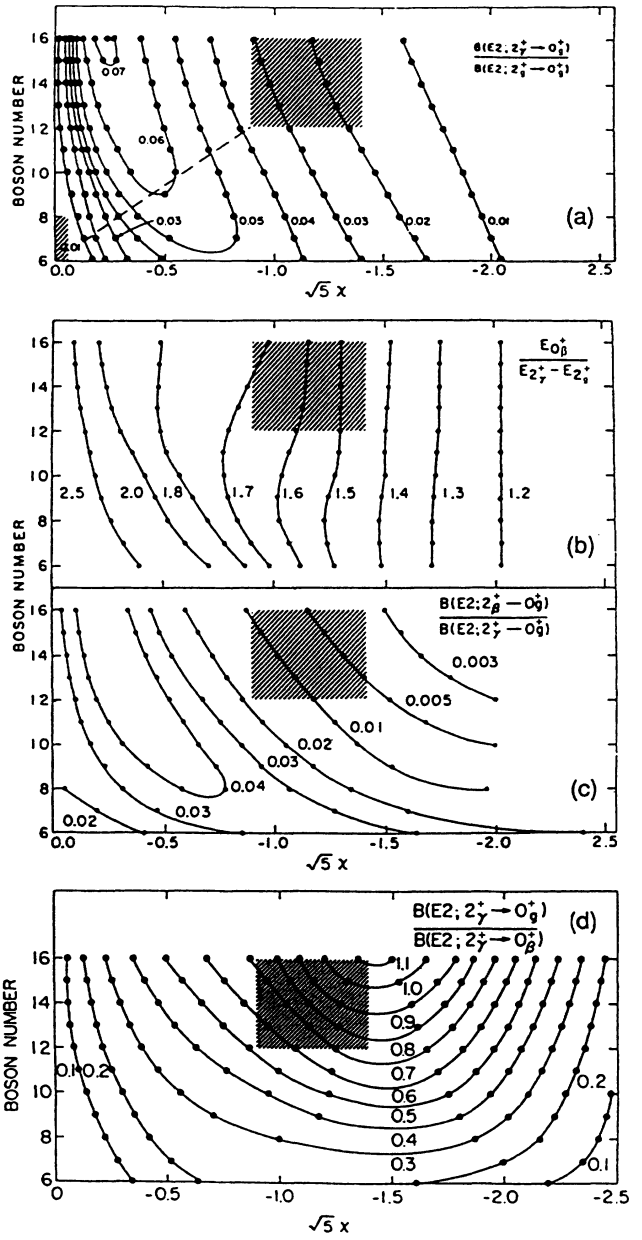

FIG. 7. Several contour plots of various observables against χ and N_B calculated with the Hamiltonian $H = -\kappa Q \cdot Q$ in the CQF. From Ref. [12]. Note the extra factor of $\sqrt{5}$ on the abscissa (retained here for historical reasons): as a consequence SU(3) corresponds to $\sqrt{5}\chi = -2.958$ and typical deformed nuclei have $\sqrt{5}\chi \sim -1.1$.

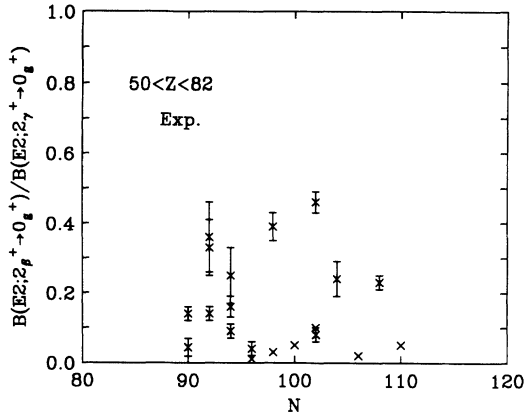

FIG. 8. Empirical values of the indicated $B(E2)$ ratio. The IBA [see Fig. 7(c)] predicts that this ratio is $\ll 1$, in agreement with the data. Updated from Ref. [12].

magnitude or more larger than expected, is of collective magnitude, and is at variance with traditional concepts of β band structure.

Relation (3) reflects a well-known empirical result that the IBA automatically exhibits. The data are shown in Fig. 8. Although there is scatter in the data, all the ratios are well below unity and most are ≤ 0.2. The numerical IBA predictions shown in Fig. 7(c) are generally smaller than the data but the inherent prediction that $B(E2 : \beta \rightarrow g)/B(E2 : \gamma \rightarrow g) \ll 1$ agrees with the empirical situation.

Since the β and γ modes belong to the same intrinsic representation of SU(3), namely $[2N_B - 4, 2]$, and since SU(3) breaking for typical deformed nuclei depends on only the single parameter χ, there must *necessarily* be a relation in the IBA between the properties of the lowest excited $K = 0$ and 2 vibrations in the IBA. Such a linkage is absent from nearly all geometric models and even from many microscopic treatments of traditional $K = 0$ and 2 quadrupole vibrations. The β-γ linkage shows up in the IBA in two related ways, both of which can be tested empirically. First, it implies that the $E2$ decay properties of the γ band are inextricably linked to the energy of the β band. This unfamiliar conclusion means that observables such as

$$\frac{B(E2 : 2^+_\gamma \rightarrow 0^+_g)}{B(E2 : 2^+_\gamma \rightarrow 2^+_g)} \quad \text{and} \quad \frac{E(2^+_\beta)}{E(2^+_\gamma)}$$

are related, that is, in effect, that such quantities as absolute $\gamma \leftrightarrow g$ $E2$ matrix elements and the β/γ vibrational energy ratio are linked. This is in fact observed experimentally as shown in Fig. 9. While there is certaintly some scatter in the data there is equally clearly a correlation. Moreover, the trend of the empirical relation, that $B(E2 : 2^+_\gamma \rightarrow 0^+_g)/B(E2 : 2^+_\gamma \rightarrow 2^+_g)$ decreases with increasing $E(2^+_\beta)/E(2^+_\gamma)$, is the same as predicted by the IBA for nuclei undergoing the structural change from well-deformed $[\sqrt{5}\chi \sim -1.1, N_B \sim 16]$ toward O(6) $[\sqrt{5}\chi = 0, N_B \sim 6]$ (upper middle to lower left in Fig. 7) that occurs in the second half of the rare-earth region. This is shown by the solid curve in Fig. 9 which gives the IBA prediction for the straight-line trajectory of χ and N_B values shown in Fig. 7(a). Although this schematic calculation represents the simplest trajectory, the curve reproduces the data quite well.

Having established the IBA prediction of a conceptual correlation of β- and γ-band properties, we can now go one step further and ask if the *specific numerical* values of E_β/E_γ predicted by the IBA are reasonable. We note

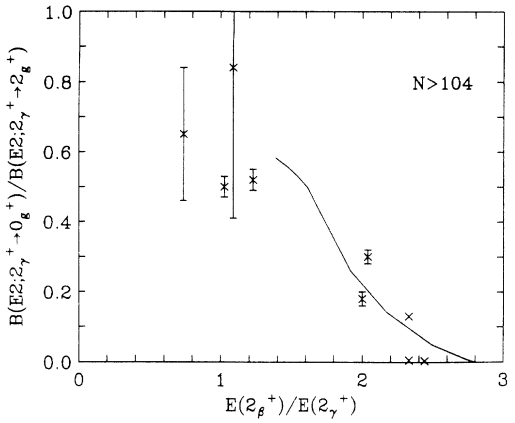

FIG. 9. Empirical correlation between a $\gamma \to g$ band $B(E2)$ ratio and the energy of the β band relative to the γ band. The IBA predicts that these two observables are correlated. The solid curve shows the IBA prediction for the linear sequence of χ and N_B values spanning an SU(3)↔O(6) transition region indicated in Fig. 7(a).

immediately from Fig. 7(b) that, for reasonable χ values for deformed nuclei, the IBA unavoidably predicts that E_β/E_γ lies in the range 1.2–1.8. The reason these ratios are slightly above unity is simple. The β and γ bands are degenerate in SU(3) and, as noted above, the principal effect of SU(3) breaking is $\Delta K = 0$ mixing in which the β and g bands repel, forcing the β band above the γ band. The greater the SU(3)-breaking terms in the Hamiltonian, the larger the $\Delta K = 0$ mixing and the higher the β band is pushed, raising the E_β/E_γ ratio. Figure 10 shows that for the vast majority of deformed nuclei the experimental ratios also range from about 0.8 to 1.7, in good agreement with the IBA predictions. Given that nothing relating directly to this energy ratio need go into the choice of IBA parameters and that, in principle, the predicted ratio could take on virtually any values, this concurrence is remarkable. Indeed, the figure itself shows that E_β/E_γ values near unity are not somehow a trivial result or a universal phenomenon: in *nondeformed* nuclei, this energy ratio can and does differ greatly from unity. In harmonic U(5), for example, the ratio is 2.0, in anharmonic U(5) calculations it is invariably > 2.0, and, in O(6), the $\tau(\tau+3)$ term gives a ratio of 3.0 for the $\sigma = N_B, \tau = 3$ 0^+ state while the β/γ energy ratio is even higher if the $\sigma = N_B - 2, \tau = 0$ 0^+ state is used for the comparison. Such values $\gtrsim 2$ are indeed seen empirically on the flanks of the deformed region in Fig. 10.

The discussion in this section perhaps supports a different picture of what we have called the "β vibration," that is, the lowest excited $K = 0$ band, than is customary. All the points would be more consistent with a description of this excitation as (at least partly) a double γ mode: it has an energy between one and two times E_γ, it has collective $B(E2)$ values to the γ band and very small $B(E2)$ values to the ground band, and, in general, its properties are linked (both empirically and in the IBA) to those of the γ band. The IBA description of the lowest excited $K = 0$ band, which agrees with its observed properties, seems to show such a character, at least for finite N_B and realistic [broken-SU(3)] calculations. Although the nature of this $K = 0^+$ band is still an open question, it is clear that the IBA has played an important role in elucidating the structure of one of the two most studied and prolific low-energy collective modes in nuclei.

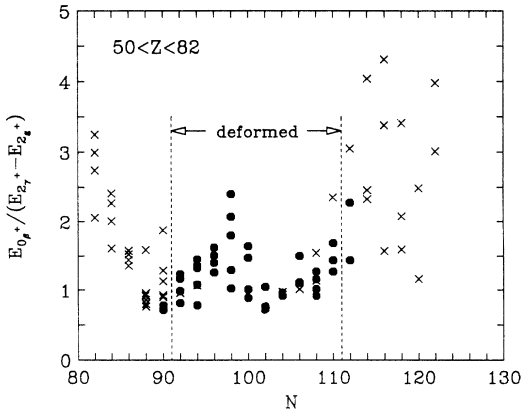

FIG. 10. Empirical energy ratios of β to γ-band energies. Data from Ref. [24]. The region of deformed nuclei is indicated by vertical dashed lines. Solid dots denote nuclei with $E(4_1^+)/E(2_1^+) \geq 3.0$ (i.e., deformed nuclei). Crosses denote other nuclei. Most of the values for deformed nuclei are in the range 0.8–1.7 which is the same range as inherently predicted, for deformed nuclei, in the IBA [see Fig. 7(b)]. The IBA predicts higher ratios for other types of structures, for example, 2.0 for the harmonic U(5) limit and 3.0 for the lowest 0^+ state in O(6). The data reflect these higher values on the left and right sides of the deformed region in the figure, respectively.

D. Transition regions

While the detailed behavior of observables across phase transitions from one symmetry toward another in the IBA depends on specifics of the calculations, there are a number of generic properties of the systematics. The best examples refer to observables, such as $B(E2: 2_\gamma^+ \to 0_g^+)$ values, or branching ratios such as $B(E2: 3_1^+ \to 2_1^+)/B(E2: 3_1^+ \to 2_2^+)$, which are zero in each symmetry and finite *only* in transition regions. They thus *must* show a "bell-shaped" dependence across a span of nuclei between two symmetries. A similar result may also apply to other valence models and is deserving of further study. The IBA prediction is illustrated in Fig. 7(a) where one sees that it is impossible to go from O(6) [$\sqrt{5}\chi = 0$, low N_B] to SU(3)—or to *any* actual deformed nucleus [$\sqrt{5}\chi \sim -1.1, N_B \gtrsim 12$] without the ratio illustrated passing through a maximum. (The same prediction is true for many other observables.) Figure 11 illustrates the experimental situation for the $B(E2)$ ratio of Fig. 7(a) and indeed shows that the predicted bell shape is observed. The solid line in the figure is the *simplest possible* IBA prediction, namely, that corresponding to the straight dashed line in Fig. 7(a) from O(6) to

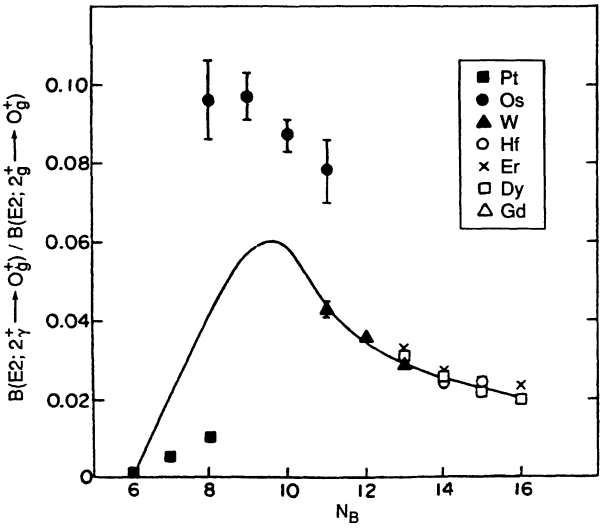

FIG. 11. Empirical $B(E2 : 2_\gamma^+ \rightarrow 0_g^+)/B(E2 : 2_g^+ \rightarrow 0_g^+)$ values for rare-earth nuclei. In agreement with the data, the IBA predicts that this ratio, which is zero in all three dynamical symmetries, attains finite values in nuclei deviating from these IBA symmetries. The solid line is the simplest possible IBA prediction, corresponding to the dashed straight-line trajectory in Fig. 7(a). From Ref. [12].

the cross-hatched region denoting deformed nuclei near $-\sqrt{5}\chi \sim -1.1$ and $N_B \sim 16$. Even this highly schematic IBA prediction reproduces well the trend of the data. Of course, a more detailed fit to individual nuclei, especially the Os isotopes, could do better.

IV. SUMMARY

Other items could be cited, or the above could be phrased in alternate ways, but the overriding point is simple: the IBA contains a large number of inherent, automatic, intrinsic, essentially parameter-free, predictions, some of which were unexpected when first proposed, some of which are at variance with other models, and some of which (e.g., the β, γ relationship) are beyond the scope of a number of other models, but all of which are in agreement with the data. Some of these predictions may also characterize other valence models, and we encourage studies to elucidate this question: such studies may help further and better identify the essential elements that generate these features of collective behavior and systematics. Some of the IBA predictions have their origins in the character of the IBA symmetries, others reflect the effects of, and variations in, finite boson number across series of nuclei, some are reflections of the nature of symmetry-breaking mechanisms in the IBA, and some show the interplay of one or more of these features. All are inherent and robust, none can be reversed by parameter changes, and all reflect real nuclei.

ACKNOWLEDGMENTS

We are grateful to S. Pittel, F. Iachello, A. Arima, W. Nazarewicz, B. R. Mottelson, and I. Hamamoto for very useful discussions which motivated and inspired this work. Many of the points discussed here and compared with compilations of the data originally evolved in collaborations with D. D. Warner for which we are particularly thankful. Research was supported in part by Contracts No. DE-AC02-76CH00016 and DE-FG02-88ER40417 with the U.S. DOE, by the BMFT under Contract No. 06-OK-602-I, and by the IAP under Contract No. 62-93-2.

[1] A. Arima and F. Iachello, Phys. Rev. Lett. **35**, 1069 (1975).
[2] A. Arima and F. Iachello, Ann. Phys. (N.Y.) **99**, 253 (1976); **111**, 201 (1978); **123**, 468 (1979); F. Iachello and A. Arima, *The Interacting Boson Model* (Cambridge University Press, Cambridge, 1987); F. Iachello and A. Arima, Phys. Rev. Lett. **40**, 385 (1978).
[3] J. A. Cizewski *et al.*, Phys. Rev. Lett. **40**, 167 (1978).
[4] O. Scholten, F. Iachello, and A. Arima, Ann. Phys. (N.Y.) **115**, 325 (1978).
[5] D. D. Warner, R. F. Casten, and W. F. Davidson, Phys. Rev. Lett. **45**, 1761 (1980).
[6] See R. F. Casten and D. D. Warner, Rev. Mod. Phys. **60**, 389 (1988); R. F. Casten, P. O. Lipas, D. D. Warner, T. Otsuka, K. Heyde, and J. P. Draayer, in *Algebraic Approaches to Nuclear Structure*, edited by R. F. Casten (Harwood Academic, Langhorne, PA, 1993), Chap. 3.
[7] A. Arima, T. Otsuka, F. Iachello, and I. Talmi, Phys. Lett. **66B**, 205 (1977).
[8] T. Otsuka, A. Arima, and F. Iachello, Nucl. Phys. **A309**, 1 (1978).
[9] P. von Brentano, A. Gelberg, H. Harter, and P. Sala, J. Phys. G **11**, L85 (1985).
[10] D. Bohel *et al.*, Phys. Lett. **137B**, 27 (1984); A. Richter, Nucl. Phys. **A522**, 139c (1991); P. O. Lipas, P. von Brentano, and A. Gelberg, Rep. Prog. Phys. **53**, 1355 (1990).
[11] R. F. Casten and P. von Brentano, Phys. Lett. **152B**, 22 (1985).
[12] D. D. Warner and R. F. Casten, Phys. Rev. Lett. **48**, 1385 (1982).
[13] A. Barfield, B. R. Barrett, J. L. Wood, and O. Scholten, Ann. Phys. (N.Y.) **182**, 344 (1988); W.-T. Chou, R. F. Casten, and N. V. Zamfir, Phys. Rev. C **45**, R2545 (1992).
[14] N. V. Zamfir, O. Scholten, and P. von Brentano, Z. Phys. A **337**, 293 (1990).
[15] O. Castanos and J. P. Draayer, Nucl. Phys. **A491**, 349

(1989); C. L. Wu *et al.*, Phys. Lett. **168B**, 313 (1986).
[16] S. Raman *et al.*, At. Data Nucl. Data Tables **36**, 1 (1987).
[17] J. N. Ginocchio and M. W. Kirson, Nucl. Phys. **A350**, 31 (1980).
[18] A. S. Davydov and G. F. Filippov, Nucl. Phys. **8**, 237 (1958).
[19] N. V. Zamfir and R. F. Casten, Phys. Lett. B **260**, 265 (1991).
[20] R. F. Casten, D. D. Warner, and A. Aprahamian, Phys. Rev. C **28**, 894 (1983).
[21] R. F. Casten and D. D. Warner, Phys. Rev. Lett. **48**, 666 (1982).
[22] R. F. Casten, A. Aprahamian, and D. D. Warner, Phys. Rev. C **29**, 356 (1984).
[23] O. Castanos, A. Frank, and P. van Isacker, Phys. Rev. Lett. **52**, 263 (1984).
[24] M. Sakai, At. Data Nucl. Data Tables **31**, 399 (1984).